Chemical Science

ROYAL SOCIETY OF CHEMISTRY

EDGE ARTICLE

View Article Online
View Journal | View Issue

Cite this: *Chem. Sci.*, 2026, **17**, 1282

All publication charges for this article have been paid for by the Royal Society of Chemistry

Received 3rd November 2025
Accepted 17th November 2025

DOI: 10.1039/d5sc08516k

rsc.li/chemical-science

Raising the HOMO level of the [*closo*-$B_{10}H_{10}$]$^{2-}$ anion: apical alkyl derivatives for modern materials

Rafał Jakubowski, [ab] Kehinde Ogunmola, [c] Oleksandr Hietsoi, [b] Andrienne C. Friedli, *[b] Kevin H. Shaughnessy *[c] and Piotr Kaszyński *[abd]

The HOMO energy of the [*closo*-$B_{10}H_{10}$]$^{2-}$ anion is increased by placing one or two alkyl groups at the apical positions of the cluster. To accomplish this, a Pd(0) catalysed C–B cross coupling reaction of RZnCl and mono- or diiodo cluster derivatives was developed. DFT results show that these iodo derivatives are the most challenging substrates among typical *closo*-borane iodides characterised by the highest B–I bond strength and associated the largest σ* MO energy. The most effective catalyst for the B–I coupling reaction was BrettPhosPd-G3, which gave the alkylated products in high yields. The alkyl effect on the {B_{10}} cluster geometry was demonstrated with single crystal XRD and correlation analyses. The electronic properties of the mono- and dialkyl products were probed with electrochemistry and UV-vis spectroscopy of charge transfer ion pairs. The electrochemical results correlate with Hammett substituent parameters and DFT derived E_{HOMO}, while the CT band energy is proportional to the difference between the FMO energies. Material properties of such newly available alkyl derivatives of the [*closo*-$B_{10}H_{10}$]$^{2-}$ anion were investigated with an Fe(II) complex and ionic LCs displaying CT behaviour.

Introduction

closo-Boron clusters[1] are unique inorganic compounds that are of increasing interest, mainly as structural elements of advanced materials and pharmacophores.[2] Their geometry is suitable for self-organizing materials,[3] while the σ-aromatic electronic structure[4] can be exploited in tuning photophysical and electrochemical properties of organic materials.[5] Of the common *closo*-boron clusters, the *closo*-decaborate dianion[6] [*closo*-$B_{10}H_{10}$]$^{2-}$ (**A**, Fig. 1) is notable for its square bipyramidal geometry with D_{4d} symmetry and exceptionally high HOMO energy level. These properties make the cluster particularly attractive for the design of photonic materials with low energy bandgaps and CT behaviour.[7]

The HOMO energy of the [*closo*-$B_{10}H_{10}$]$^{2-}$ cluster responds to the electronic properties of the substituents,[7] with electron-donating groups increasing its level. Most substituents investigated to date are electron withdrawing, while those with electron donating properties are needed for achieving the full range of tuneable electronic properties of anion **A**. Unfortunately, the negative charge on the [*closo*-$B_{10}H_{10}$]$^{2-}$ cluster increases the basicity of typical π-electron-donating atoms, such as X = O and N, which leads to their ready protonation and consequent lowering of the HOMO energy level. One substituent that has a moderately negative σ_p parameter[8] (−0.16), yet lacks basic sites, is the alkyl group. The only example of an apical alkyl derivative of anion **A** is the dimethyl derivative [*closo*-$B_{10}H_8$-1,10-Me_2]$^{2-}$ obtained by $LiAlH_4$ reduction of the dicarbonyl derivative [*closo*-$B_{10}H_8$-1,10-$(CO)_2$].[9] Further exploration of this class of compounds as electron donors, liquid crystals and photonic materials with tuneable properties requires a more general method for controlled and regioselective substitution of alkyl groups onto the [*closo*-$B_{10}H_{10}$]$^{2-}$ anion. In this report we demonstrate selective preparation of mono and di-alkyl derivatives substituted at the apical positions of [*closo*-$B_{10}H_{10}$]$^{2-}$ anion (Fig. 1).

A potential general route to apical mono- or dialkyl-substituted [*closo*-$B_{10}H_{10}$]$^{2-}$ anions, **1** and **2** in Fig. 1, would be palladium-catalysed alkylation and dialkylation of the previously reported iodides[10] [*closo*-$B_{10}H_9$-1-I]$^{2-}$ (**3**) and [*closo*-

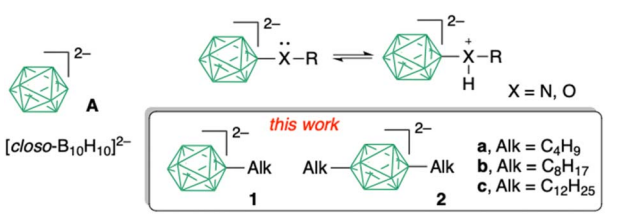

Fig. 1 Left: [*closo*-$B_{10}H_{10}$]$^{2-}$ (**A**). Right: protonation of RX derivative of [*closo*-$B_{10}H_{10}$]$^{2-}$. In the box: apical alkyl derivatives of anion **A**. In the cluster each unsubstituted vertex corresponds to a B–H fragment.

[a]*Centre of Molecular and Macromolecular Studies, Polish Academy of Sciences, 90-363 Łódź, Poland. E-mail: piotr.kaszynski@cbmm.lodz.pl*

[b]*Department of Chemistry, Middle Tennessee State University, Murfreesboro, TN 37132, USA*

[c]*Department of Chemistry and Biochemistry, The University of Alabama, Tuscaloosa, AL 35487, USA*

[d]*Faculty of Chemistry, University of Łódź, 91-403 Łódź, Poland*

$B_{10}H_8$-1,10-$I_2]^{2-}$ (**4**), respectively. Palladium-catalysed B–C bond formation (alkylation, arylation and alkynylation reactions) is fairly well established for iodo derivatives of *closo*-$C_2B_{10}H_{12}$,[11] and to a lesser extent for anions [*closo*-1-$CB_{11}H_{12}]^-$,[12] [*closo*-$B_{12}H_{12}]^{2-}$,[13] and [*closo*-1-$CB_9H_{10}]^-$,[14] but all these reactions are limited in scope compared to the analogous C–C cross-coupling. For derivatives of [*closo*-$B_{10}H_{10}]^{2-}$ (**A**) there are only three reported examples of Kumada coupling of aryl Grignard reagents with iodides **3** and **4**.[7b,10] No palladium-catalysed alkylation or alkynylation reactions of anion **A** to give apically substituted *closo*-borate derivatives have been reported to date.[9b]

Herein we report an efficient Pd(0)-catalysed alkyl-B cross-coupling in [*closo*-$B_{10}H_{10}]^{2-}$ anion, and preparation of derivatives **1** and **2** containing three representative alkyl groups, butyl (**a**), octyl (**b**) and dodecyl (**c**, Fig. 1). The effect of the alkyl group on the structural and electronic properties of anion **A** is investigated with XRD, spectroscopic, electrochemical and DFT methods. Monoalkyl derivatives are used to prepare an Fe(II) complex and to test for the formation of ionic liquid crystals with intermolecular charge transfer properties.

Results and discussion

Analysis of electrophile electronic properties

Oxidative addition of a carbon–halogen bond to a Pd(0) centre is the first step in palladium-catalyzed cross-coupling reactions.[15] Such additions of haloarenes to Pd(0) are thermodynamically favourable leading to isolable complexes. The rate of the process decreases with increasing bond strength (rate: I > Br > Cl)[16] and correlates with the energy of the C–X σ* molecular orbital. Oxidative addition of B–X bonds of *closo*-boranes is significantly more challenging than for aryl halide C–X bonds due to the high strength of the B–X bond and the increased energy level of the associated orbital. For example, reaction of 9-iodo-*m*-carborane with $Pd(PPh_3)_4$ in toluene at 70 °C for 3 h resulted in no observable reaction when analysed by ^{31}P NMR spectroscopy.[17] When the reaction of 9-iodo-*m*-carborane with $Pd(PPh_3)_4$ was performed in the presence of $[Bu_4N]Br$ for 12 h at 30 °C and then 2 hours at 55 °C, a 1 : 5 ratio of 9-bromo-*m*-carborane and 9-iodo-*m*-carborane was obtained. This result suggests that oxidative addition of the B–I bond of carborane occurs as part of a reversible endothermic step, in which the concentration of the oxidative addition product is below the ^{31}P NMR detection limit. The subsequent halide exchange at the Pd centre followed by reductive elimination gives the B–Br product. Presumably, successful palladium-catalysed functionalization of iodo-*closo*-boranes proceeds through a similar reversible endothermic oxidative addition of the B–X bond to Pd(0) and trapping of the transient Pd(II)-boryl intermediate by the coupling partner.

DFT calculations at the B3LYP/Def2TZVP level of theory demonstrate that the B–I bond of all the *closo*-borate clusters are significantly stronger (by 12–34 kcal mol^{-1}) than the C–I bond of iodobenzene, and the bond strength increases with increasing negative charge on the cluster (red bars in Fig. 2). The B–I bond is also stronger for the 10-vertex clusters

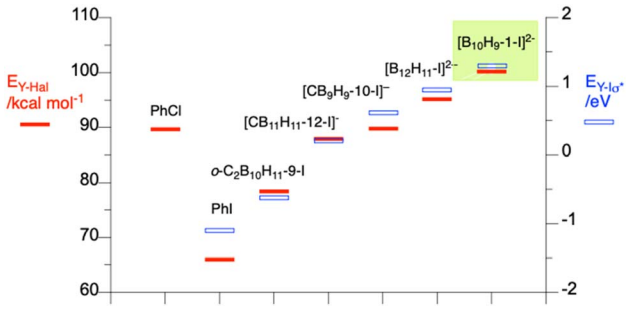

Fig. 2 DFT (B3LYP/Def2TZVP) calculated homolytic BDE ($E_{Y\text{-}Hal}$, red bars) and B/C–I σ* orbital energies (blue hollow bars) in the gas phase. For details see SI.

compared to the 12-vertex analogue (*e.g.* [*closo*-$B_{12}H_{11}$-1-$I]^{2-}$ *vs.* [*closo*-$B_{10}H_9$-1-$I]^{2-}$). It should be noted that the B–I bond in the [*closo*-$B_{10}H_9$-1-$I]^{2-}$ cluster is about 9 kcal mol^{-1} stronger than the C–Cl bond of chlorobenzene, which is already a demanding substrate for Pd-catalysed cross-coupling. A similar trend is found for the energy associated with the B–I σ* orbital (blue bars in Fig. 2), which would be the key orbital involved in oxidative addition. Results show that the B–I σ* energy for [*closo*-$B_{10}H_9$-1-$I]^{2-}$ anion (**3**) is the highest in the series: it is nearly 2.4 eV higher than that of the C–I σ* in iodobenzene or 1.9 eV higher than the B–I σ* in iodocarborane. Thus, the calculated highest B–I bond strength and σ* energy in the series for **3** suggest that oxidative addition of the dianionic iodide **3** to Pd(0) centre will be particularly difficult. It was hypothesized that successful cross-coupling of derivatives of [*closo*-$B_{10}H_{10}]^{2-}$ (**A**) would require a palladium catalyst that is highly activated towards oxidative addition and conditions to promote fast transmetalation of the transient palladium-boryl intermediate present in low concentrations.

Synthetic method development

Initial optimization of the C–B cross-coupling reaction conditions was performed for butylzinc chloride, generated *in situ* from butylmagnesium chloride and $ZnCl_2 \cdot LiCl$, and [*closo*-$B_{10}H_8$-1,10-$I_2][Bu_4N]_2$ (**4[Bu$_4$N]**, Scheme 1). Palladium catalyst systems known to promote coupling with less reactive aryl halides[18] were tried first.[19] PEPPSI-IPr, G3-XPhos, and G3-DPPF gave no conversion to the alkylated product and produced only the hydrodeiodinated parent **A** in addition to unreacted iodide **4[Bu$_4$N]**. Byproduct **A** is likely formed by β-hydrogen elimination

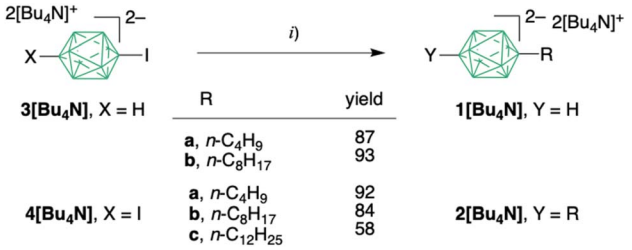

Scheme 1 Synthesis of mono and dialkyl derivatives **1** and **2**.[a] Reagents and conditions: (i) $RMgCl/ZnCl_2/LiCl$ (10 eq per B–I), BrettPhosPd-G3 (3.75 mol% per B–I), THF, reflux, 72 h.

of palladium alkyl intermediates to give a boryl-palladium hydride that undergoes reductive elimination to give the B–H bond. In contrast, catalysts derived from BrettPhos or SPhos and the G3 palladacycle precatalyst gave full consumption of **4** and low yields of the desired product **2a** (~25%) accompanied by a complex mixture of boron byproducts, including **1a** and the parent **A**. The reactions were followed by ^{11}B NMR, where the characteristic peaks of the apical boron atoms were shifted from about −5 ppm in the starting iodide to about 5 ppm in the alkylated products.[19] Full details and summary of all experiments are provided in the SI.

It was reasoned that the poor selectivity for the alkylated product with BrettPhos and SPhos may be partially due to inefficient interception of the palladium-boryl intermediate by the organozinc reagent, which allows unproductive processes to occur with the palladium-boryl species. Increasing the ratio of the organozinc reagent to the boron cluster improved the selectivity for the dialkylated product with the BrettPhos-G3 catalyst system. With a 20 : 1 mole ratio of butylzinc chloride to **4[Bu$_4$N]**, 92% conversion to [*closo*-$B_{10}H_8$-1,10-Bu_2]$^{2-}$ **2a** was achieved after 72 hours with only traces of [*closo*-$B_{10}H_{10}$]$^{2-}$ and [*closo*-$B_{10}H_9$-1-Bu]$^{2-}$ as byproducts based on ^{11}B NMR spectroscopy.

Under these conditions, BrettPhos was the optimal ligand. Lower yields of **2a** were obtained using SPhos, CPhos, or JoyPhos with the G3 palladacycle. Rigorous exclusion of oxygen in all stages of preparation of **2a** by setting up the reactions under nitrogen in the glove box was critical to the success of the reaction. The subsequent work-up and purification of the products was conducted in air on the benchtop. Reactions set up under Ar on the benchtop using standard anaerobic techniques gave complex mixtures with no desired product.

Using these optimized conditions, [*closo*-$B_{10}H_8$-1,10-Bu_2][Bu$_4$N]$_2$ (**2a[Bu$_4$N]**) was isolated in 92% yield with >90% purity (^{11}B NMR) after aqueous workup in air and purification using a short alumina column (Scheme 1). The product was isolated as an oil that solidified upon standing. The dioctyl **2b[Bu$_4$N]** and didodecyl **2c[Bu$_4$N]** analogues were isolated in 84% and 58% yield, respectively, and purity >90%. Mono-alkylated products, monobutyl **1a[Bu$_4$N]** and monooctyl **1b[Bu$_4$N]** were obtained in high yields starting from [*closo*-$B_{10}H_9$-1-I][Bu$_4$N]$_2$ (**3[Bu$_4$N]**) and using a 10 : 1 mole ratio of the organozinc reagent to the iodide.

Attempts were made to convert the oily or waxy [Bu$_4$N]$^+$ salts of **1** and **2** to easier-to-handle and more oxidatively stable crystalline derivatives, such as those containing the [Et$_4$N]$^+$ or Cs$^+$. Thus, extraction of **2a[H$_3$O]** to ether from 10% HCl solution of **2a[Bu$_4$N]** followed by treatment with [Et$_4$N]Cl gave the desired **2a[Et$_4$N]** along with approximately 50% decomposition products, as demonstrated[19] by complex ^{11}B NMR spectra (see the SI). Attempted cation exchange using ion exchange resins gave incomplete ion exchange and partial decomposition. It was determined that all dialkylated and, to lesser extent, mono-alkylated products are acid-sensitive, possibly due to their elevated HOMO level leading to facile protonation of the cage and presumably ring opening to *nido* derivatives.[20] Therefore, the oily [Bu$_4$N]$^+$ salts were used for further transformations. For crystallographic characterisation, two ion pairs of mono- and di-butyl derivatives **1a[Ph$_4$P]** and **2a[Ph$_4$P]** were obtained by metathesis of the [Bu$_4$N]$^+$ salts with [Ph$_4$P]Cl in CH_2Cl_2/H_2O system.

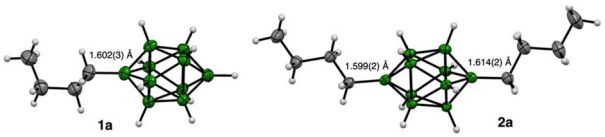

Fig. 3 Thermal ellipsoid diagram for anions **1a** and **2a** (ellipsoids set at 50% probability) with the [Ph$_4$P]$^+$ cations and solvent molecule omitted for clarity. Angle between the alkyl group mean planes in **2a** is 28.8°. For details see the SI.

Molecular and crystal structures

Single crystals of ion pairs **1a[Ph$_4$P]·MeOH** (monoclinic, $P2_1/n$) and **2a[Ph$_4$P]** (triclinic, $P\bar{1}$) suitable for XRD analysis were obtained by cooling followed by slow evaporation of hot MeOH solutions. Structural analysis revealed that in **1a** the Bu group adopts a staggered orientation relative to the cage, with the B(1)–C bond length of 1.602(3) Å (Fig. 3). The C(2)–C(3) bond in the butyl chain exists in a gauche conformation. In the dibutyl derivative **2a**, the alkyl groups in the all-*trans* conformation are rotated about 8° from the ideal eclipsed orientation, with B–C distances of 1.599(2) and 1.614(2) Å, respectively. These distances are well reproduced by DFT calculations (1.608 Å) and are similar to that found in a B(10)–alkyl derivative of the [*closo*-1-CB_9H_{10}]$^-$ anion (1.593(3) Å).[14a]

Further structural analysis indicates that the Bu groups in **1a** and **2a** exert a significant effect on the {B_{10}} cage geometry. Thus, the height of the tetragonal pyramid (1.116 Å) and the resulting B(1)···B(10) separation in **2a** (3.757(2) Å), are the largest reported to date for apical derivatives of **A**, and consistent with the strong electron donating character of the apical substituent. In a series of nine [*closo*-$B_{10}H_8$-1,10-X_2]$^{2-}$ derivatives,[7b,21] including **2a**, both distances correlate well ($r^2 > 0.95$) with Hammett[8] substituent parameters σ_p giving the slope of 0.054(4) and 0.12(1) Å/σ_p, respectively.[19]

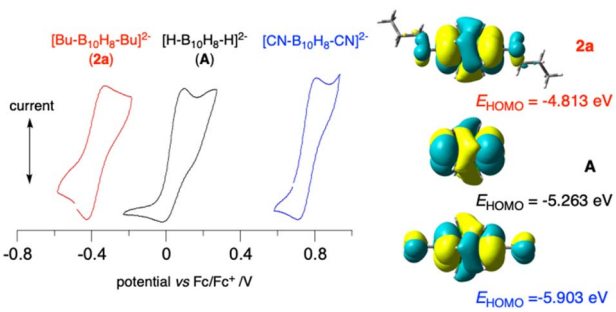

Fig. 4 Left: cyclic voltammograms for dibutyl **2a[Bu$_4$N]** (red), parent **A** (black) and [*closo*-$B_{10}H_8$-1,10-$(CN)_2$]$^{2-}$ (blue). Conditions: 0.5 mM analyte in MeCN [Bu$_4$N][PF$_6$] (100 mM) at *ca* 22 °C, scans of 100 mV s^{-1} in the anodic direction, glassy carbon working electrode ($\varphi = 1$ mm), Pt counter electrode and an Ag/AgCl pseudo-reference electrode. Right: B3LYP/Def2TZVP-derived HOMO contours and energies in MeCN dielectric medium (MO Isovalue = 0.02). Full data in SI.

Electrochemical analysis

The effect of the alkyl groups on the level of the HOMO of the $\{B_{10}\}$ cage was probed with electrochemical methods. Cyclic voltammetry demonstrated that the oxidation processes in **1a** and **2a** recorded in MeCN are quasireversible and significantly more cathodic than those of the parent dianion **A** by 0.19 V and 0.42 V (Fig. 4 and ESI). This shift corresponds to lifting the HOMO of dianion **A** by 0.23 and 0.45 eV, respectively, or lowering the adiabatic ionisation energy by 0.30 and 0.52 eV, respectively, according to DFT calculations in MeCN dielectric medium.[19] The measured low oxidation potential $E_{1/2}^{0/+1}$ of −0.376 V *vs.* the Fc/Fc^+ couple for **2a[Bu$_4$N]** is consistent with the observed limited stability of this and other dialkyl derivatives **2** during storage, presumably due to air oxidation and sensitivity to acids.

Analysis of a series of eight $[closo\text{-}B_{10}H_8\text{-}1\text{-}X\text{-}10\text{-}Y]^{2-}$ derivatives containing apical Bu, CN and Ar substituents demonstrates a good correlation of $E_{1/2}^{0/+1}$ with the sum of Hammett[8] substituent parameters, $\Sigma\sigma_p$ (Fig. 5), and excellent correlation with the calculated HOMO level and adiabatic ionisation energy for each anion.[19] Assuming validity of this correlation in Fig. 5, the $E_{1/2}^{0/+1}$ potential of the hypothetical 1,10-dimethoxy derivative $[closo\text{-}B_{10}H_8\text{-}1,10\text{-}(OMe)_2]^{2-}$ can be predicted to be −0.49(2) V *vs.* the Fc/Fc^+ couple, while its B(1)···B(10) separation would be 3.76(1) Å.

Charge transfer complexes

The high level of the HOMO in alkyl derivatives **2** is also evident from energies of intermolecular charge transfer (CT) bands observed in concentrated solutions of ion pairs of **2b** with pyridinium cations (Fig. 6, Chart 1). Thus, as the electron-withdrawing power of the C(4) substituent on the *N*-alkylpyridinium cation increases, the LUMO energy decreases, and so does the difference, ΔE_{FMO}, between the energies of the LUMO of pyridinium and the HOMO localized on the anion. Consequently, the energy of the intermolecular CT band decreases from 2.33 eV (532 nm) for **2b[PyrCOOC$_{11}$]** to 2.05 eV (604 nm) for **2b[Q12]** (see structures in Chart 1). These experimental CT energies correlate well with the calculated ΔE_{FMO} values (Fig. 6), as observed previously for related ion pairs, *e.g.* **5[PyrCN]** and **6[PyrCN]** in Chart 1.[7b] As expected, the CT band of **2b[PyrCN]** is positioned between those of the two analogous ion pairs, the dicarboxylate **5[PyrCN]** and dialkoxyphenyl **6[PyrCN]** (Fig. 6, left).

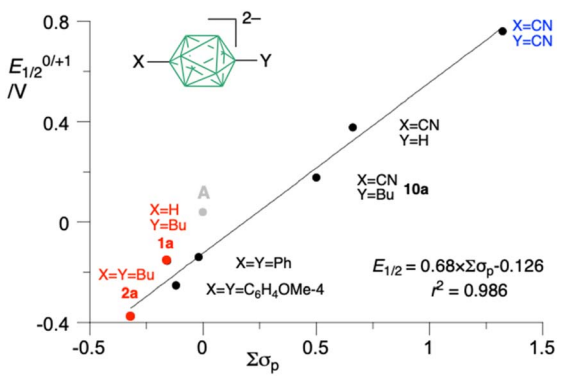

Fig. 5 Correlation of oxidation potentials $E_{1/2}^{0/+1}$ (*vs.* Fc/Fc^+) with the sum of Hammett parameters $\Sigma\sigma_p$. The datapoint for **A** (grey dot) is not used for the correlation. Numerical values are shown in the SI.

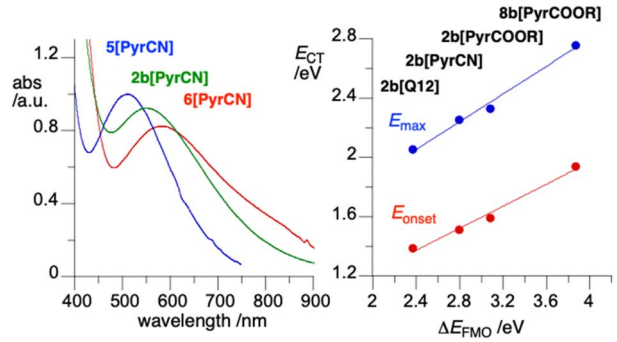

Fig. 6 Left: UV-vis spectra for ion pairs with *N*-decyl-4-cyanopyridine (**PyrCN**). Right: correlation of CT energy *vs.* difference of the FMO energies ($\Delta E_{FMO} = E_{LUMO} - E_{HOMO}$) calculated at the CAM-B3LYP/Def2TZVP level in CH_2Cl_2. See Chart 1 for structures.

Molecular materials

Polarised light optical microscopy demonstrated that none of the investigated ion pairs of anion **2b** exhibited liquid crystalline behaviour, which is in contrast to behaviour of similar ion pairs **5[PyrCN]** and **6[PyrCN]**.[7b] To induce mesogenic behaviour, the monooctyl derivative **1b** was substituted with a 4-heptyloxypyridinium group using the previously developed aryliodonium method for selective activation of B–H bonds in *closo*-borates.[12e,22] Thus, the monooctyl derivative **1b** was reacted with $PhI(OAc)_2$ in MeCN (Scheme 2) giving crude product **7b** with ~80% purity (based on ^{11}B NMR). The crude product was purified by rapid chromatography using a SiO_2 column impregnated with $[Bu_4N][HSO_4]$ to give pure, moderately stable phenyliodonium derivative **7b** in about 50% yield as a yellow-brownish oil.

The octyl derivative **7b[Bu$_4$N]** was reacted with neat 4-heptyloxypyridine to give essentially colourless product **8b[Bu$_4$N]** in 58% yield (Scheme 2). Exchange of the $[Bu_4N]^+$ cation for pyridinium **PyrCOOC$_6$** or **PyrCOOC$_{11}$** (Chart 1) gave a reddish-orange waxy solid ion pair **8b[PyrCOOC$_n$]**, which upon heating displayed textures characteristic for a smectic A phase (Scheme 2). Both ion pairs exhibited limited thermal stabilities and slowly decomposed above 150 °C, with estimated clearing temperatures below 200 °C for $n = 11$ and about 250 °C for $n = 6$.

Lastly, the significant electron donating ability of the apical alkyl group was demonstrated in Fe(II) complex **9a[Bu$_4$N]**, which

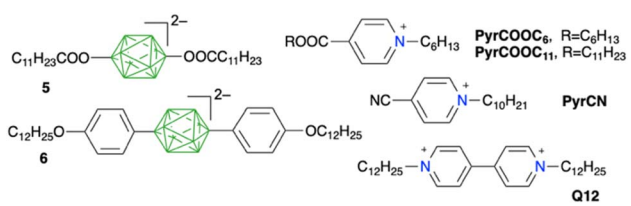

Chart 1

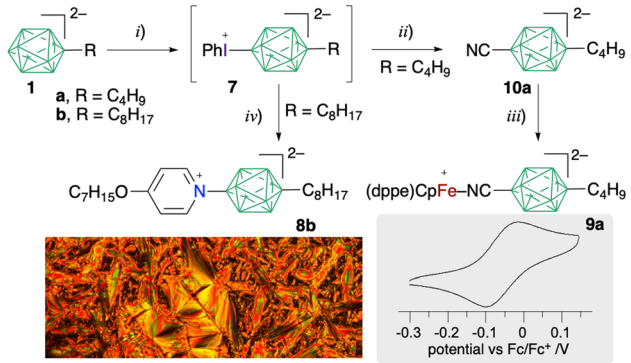

Scheme 2 Synthesis of pyridinium derivative **8b** and Fe(II) complex **9a**.[a] Reagents and conditions: (i) $PhI(OAc)_2$, MeCN, 0 °C 1 h, then rt 16 h, 45% for **7a** and 54% yield for **7b**; (ii) $[Bu_4N]CN$, MeCN, 55–60 °C, 2 d, 30% yield; (iii) $[(\eta^5\text{-Cp})(dppe)FeCl$, CH_2Cl_2, reflux 16 h, 66% yield; (iv) 4-$C_7H_{15}OC_5H_4N$ neat, 50 °C, 2 d, 58% yield. Below left: polarised optical microscopy of a Sm texture at 125 °C of **8b[PyrCOOC$_{11}$]**. Right: cyclic voltammogram for **9a[Bu$_4$N]**.

was obtained from [*closo*-$B_{10}H_8$-10-Bu-1-CN]$^{2-}$ (**10a[Bu$_4$N]**) prepared from phenyliodonium derivative **7a[Bu$_4$N]** shown in Scheme 2. Electrochemical analysis, conducted in CH_2Cl_2 for comparison purposes, demonstrated a quasireversible oxidation process with $E_{1/2}{}^{0/+1} = -0.054$ V (*vs.* Fc/Fc$^+$, Scheme 2), which is significantly cathodically shifted relative to the symmetric derivative [*closo*-$B_{10}H_8$-1,10-(CN{Fe})$_2$] (0.056 V *vs.* Fc/Fc$^+$)[23] and the analogous Fe(II) complex with pyrazinium derivative [*closo*-$B_{10}H_8$-1-CN{Fe}-10-Pyrazine] (0.080 V *vs.* Fc/Fc$^+$).[24] The observed trend in $E_{1/2}{}^{0/+1}$ values correlates well with the HOMO energy, as calculated with a DFT method (B3LYP/Def2SVP) for model compounds.[19]

Conclusions

We have demonstrated an efficient method for preparation of mono- and dialkyl derivatives of [*closo*-$B_{10}H_{10}]^{2-}$ anion (**A**) using Pd(0) catalysed B–C cross-coupling with the apical mono- and diiodo precursors, respectively. This method fills a significant void in functional derivatives of the [*closo*-$B_{10}H_{10}]^{2-}$ anion and provides access to this previously unavailable class of derivatives for further studies. Results demonstrate that each apical alkyl group raises the HOMO level of the parent dianion **A** by about 0.22 eV. Since the effect is cumulative, dialkyl derivatives **2** approach the limit of oxidative stability in air and toward acids. The high level of the HOMO in **1** and **2** was confirmed by electrochemical and UV-vis methods. The former method demonstrated a cathodic shift of the $E_{1/2}{}^{ox}$ potential by about 0.2 V per each apical alkyl group, while the electronic absorption spectroscopy revealed low energy intermolecular CT bands in pyridinium ion pairs. Substituent effects on the geometry and electronic and redox behaviour of the {B_{10}} cage correlate well with Hammett parameters σ_p and DFT results, which permits the design and fine tuning of properties. The applications of the monoalkyl derivatives **1** as an Fe(II) complex and ionic liquid crystals demonstrates materials with controlled redox properties, self-organisation and CT behaviour.

Author contributions

The manuscript was written through contributions of all authors, and all authors have given approval to the final version of the manuscript.

Conflicts of interest

The authors declare no competing financial interest.

Data availability

The data supporting this article have been included as part of the supporting information (SI).

CCDC 2362917 **1a[Ph$_4$P]·MeOH** and 2362918 **2a[Ph$_4$P]** contain the supplementary crystallographic data for this paper.[25a,b]

Supplementary information (SI): data for this article, including synthetic procedures and characterisation details (NMR, UV-vis, E-chem), crystallographic data, and computational results. See DOI: https://doi.org/10.1039/d5sc08516k.

Acknowledgements

Support for this project was provided by the National Science Foundation (CHE-1214104), National Science Centre (2020/38/A/ST4/00597). RJ was supported by Bridge Funding from the College of Basic and Applied Sciences, MTSU.

References

1 (*a*) E. L. Muetterties, ed., *Boron Hydride Chemistry*, Academic Press, New York, 1975; (*b*) R. N. Grimes, *Carboranes*, Academic Press, New York, 3rd edn, 2016.
2 (*a*) N. S. Hosmane and R. Eagling, in *Handbook of Boron Science: With Applications in Organometallics, Catalysis*, Materials and Medicine, 2019; (*b*) E. Hey-Hawkins and F. Teixidor, in *Boron-Based Compounds: Potential and Emerging Applications in Medicine*, John Wiley & Sons Ltd, 2018.
3 P. Kaszynski, in *Handbook of Boron Science*, eds. N. S. Hosmane and R. Eagling, World Scientific, London, 2018, vol. 3, pp. 57–114.
4 J. Poater, C. Viñas, I. Bennour, S. Escayola, M. Solà and F. Teixidor, *J. Am. Chem. Soc.*, 2020, **142**, 9396–9407.
5 R. Núñez, M. Tarrés, A. Ferrer-Ugalde, F. Fabrizi de Biani and F. Teixidor, *Chem. Rev.*, 2016, **116**, 14307–14378.
6 I. B. Sivaev, A. V. Prikaznov and D. Naoufal, *Collect. Czech. Chem. Commun.*, 2010, **75**, 1149–1199.
7 (*a*) S. Kapuściński, M. B. Abdulmojeed, T. E. Schafer, A. Pietrzak, O. Hietsoi, A. C. Friedli and P. Kaszyński, *Inorg. Chem. Front.*, 2021, **8**, 1066–1082; (*b*) L. Jacob, E. Rzeszotarska, M. Koyioni, R. Jakubowski, D. Pociecha, A. Pietrzak and P. Kaszyński, *Chem. Mater.*, 2022, **34**, 6476–6491.
8 C. Hansch, A. Leo and R. W. Taft, *Chem. Rev.*, 1991, **91**, 165–195.
9 (*a*) W. H. Knoth, J. C. Sauer, J. H. Balthis, H. C. Miller and E. L. Muetterties, *J. Am. Chem. Soc.*, 1967, **89**, 4842–4850;

(*b*) 2-Cyclohexyl derivative was obtained by based-induced ring closure of a *nido*-decaborane(11) derivative: E. I. Tolpin, E. Mizusawa, D. S. Becker and J. Venzel, *Inorg. Chem*, 1980, **19**, 1182–1187. Also, a reaction of [*closo*-$B_{10}H_9$-2-NH_3]- with ethyleneoxide gave di B-alkylated derivative of unspecified regiochemistry: K. C. John, A. Kaczmarczyk and A. H. Soloway, *J. Med. Chem.*, 1969, **12**, 54–57.

10 E. Rzeszotarska, I. Novozhilova and P. Kaszyński, *Inorg. Chem.*, 2017, **56**, 14351–14356.

11 (*a*) D. Olid, R. Núñez, C. Viñas and F. Teixidor, *Chem. Soc. Rev.*, 2013, **42**, 3318–3336; (*b*) R. M. Dziedzic and A. M. Spokoyny, *Chem. Commun.*, 2019, **55**, 430–442; (*c*) A. Himmelspach and M. Finze, *Eur. J. Inorg. Chem.*, 2010, 2012–2024.

12 (*a*) B. Grüner, Z. Janoušek, B. T. King, J. N. Woodford, C. H. Wang, V. Všetečka and J. Michl, *J. Am. Chem. Soc.*, 1999, **121**, 3122–3126; (*b*) A. Franken, C. A. Kilner, M. Thornton-Pett and J. D. Kennedy, *J. Organomet. Chem.*, 2002, **657**, 176–179; (*c*) A. Himmelspach, G. J. Reiss and M. Finze, *Inorg. Chem.*, 2012, **51**, 2679–2688; (*d*) M. Hailmann, L. Herkert, A. Himmelspach and M. Finze, *Chem.–Eur. J.*, 2013, **19**, 15745–15758; (*e*) P. Kaszyński and B. Ringstrand, *Angew. Chem., Int. Ed.*, 2015, **54**, 6576–6581; (*f*) J. G. Pecyna, B. Ringstrand and P. Kaszyński, *Inorg. Chem.*, 2012, **51**, 5353–5359; (*g*) J. Pecyna, P. Kaszyński, B. Ringstrand, D. Pociecha, S. Pakhomov, A. G. Douglass and V. G. J. Young, *Inorg. Chem.*, 2016, **55**, 4016–4025; (*h*) A. Jankowiak, J. Kanazawa, P. Kaszynski, R. Takita and M. Uchiyama, *J. Organomet. Chem.*, 2013, **747**, 195–200; (*i*) B. Ringstrand, A. Jankowiak, L. E. Johnson, P. Kaszynski, D. Pociecha and E. Górecka, *J. Mater. Chem.*, 2012, **22**, 4874–4880.

13 (*a*) T. Peymann, C. B. Knobler and M. F. Hawthorne, *Inorg. Chem.*, 1998, **37**, 1544–1548; (*b*) R. G. Kultyshev, S. Liu, H. T. Leung, J. Liu and S. G. Shore, *Inorg. Chem.*, 2003, **42**, 3199–3207; (*c*) A. Himmelspach, M. Finze, A. Vöge and D. Gabel, *Z. Anorg. Allg. Chem.*, 2012, **638**, 512–519; (*d*) M. Schäfer, I. Krummenacher, H. Braunschweig and M. Finze, *Z. Anorg. Allg. Chem.*, 2015, **641**, 660–668; (*e*) M. K. Al-Joumhawy, J.-C. Chang, K. I. Assaf, B. S. Bassil and D. Gabel, *Chem.–Eur. J.*, 2023, **29**, e202302466.

14 (*a*) B. Ringstrand, P. Kaszynski, A. Januszko and V. G. Young, Jr., *J. Mater. Chem.*, 2009, **19**, 9204–9212; (*b*) B. Ringstrand, P. Kaszynski and H. Monobe, *J. Mater. Chem.*, 2009, **19**, 4805–4812.

15 A. Biffis, P. Centomo, A. Del Zotto and M. Zecca, *Chem. Rev.*, 2018, **118**, 2249–2295.

16 (*a*) P. Fitton and E. A. Rick, *J. Organomet. Chem.*, 1971, **28**, 287–291; (*b*) A. Jutand and A. Mosleh, *Organometallics*, 1995, **14**, 1810–1817.

17 (*a*) W. J. Marshall, R. J. Young, Jr. and V. V. Grushin, *Organometallics*, 2001, **20**, 523–533; (*b*) C. Viñas, G. Barberá and F. Teixidor, *J. Organomet. Chem.*, 2002, **642**, 16–19; (*c*) L. M. A. Saleh, R. M. Dziedzic, S. I. Khan and A. M. Spokoyny, *Chem.–Eur. J.*, 2016, **22**, 8466–8470.

18 (*a*) B. T. Ingoglia, C. C. Wagen and S. L. Buchwald, *Tetrahedron*, 2019, **75**, 4199–4211; (*b*) N. C. Bruno, M. T. Tudge and S. L. Buchwald, *Chem. Sci.*, 2013, **4**, 916–920; (*c*) C. Valente, S. Çalimisiz, K. H. Hoi, D. Mallik, M. Sayah and M. G. Organ, *Angew. Chem., Int. Ed.*, 2012, **51**, 3314–3332.

19 For details see the SI.

20 M. F. Hawthorne, I. J. Mavunkal and C. B. Knobler, *J. Am. Chem. Soc.*, 1992, **114**, 4427–4429.

21 (*a*) L. Jacob, E. Rzeszotarska, A. Pietrzak, V. G. Young, Jr. and P. Kaszyński, *Eur. J. Inorg. Chem.*, 2020, 3083–3093; (*b*) S. Kapuściński, O. Hietsoi, A. Pietrzak, A. C. Friedli and P. Kaszyński, *Chem. Commun.*, 2022, **58**, 851–854.

22 P. Kaszyński, *Aust. J. Chem.*, 2025, **78**, CH25006.

23 J. Guschlbauer, K. H. Shaughnessy, A. Pietrzak, M.-C. Chung, M. B. Sponsler and P. Kaszyński, *Organometallics*, 2021, **40**, 2504–2515.

24 R. Jakubowski, M. B. Abdulmojeed, O. Hietsoi, A. C. Friedli and P. Kaszynski, *Inorg. Chem.*, 2024, **63**, 17774–17784.

25 (*a*) CCDC 2362917, Experimental Crystal Structure Determination, 2025, DOI: **10.5517/ccdc.csd.cc2k9t4v**; (*b*) CCDC 2362918, Experimental Crystal Structure Determination, 2025, DOI: **10.5517/ccdc.csd.cc2k9t5w**.